Supplementary Materials

Proof of Theorem 1

Proof. The conclusion in Theorem 1 is directly implied by Theorem 4.1(c) in Tseng (2001), for which we need to verify a few regularity conditions as follows.

First, $\ell_0(\mathbf{z}_1, \ldots, \mathbf{z}_n, \boldsymbol{\mu}, \boldsymbol{\Omega})$ in (9) is regular at each point in its domain. This is true because $\text{dom}(\ell_0)$ is open and ℓ_0 is differentiable and all its partial derivatives exists.

Second, the sublevel set $\{(\mathbf{z}_1, \ldots, \mathbf{z}_n, \boldsymbol{\mu}, \boldsymbol{\Omega}) : \ell(\mathbf{z}_1, \ldots, \mathbf{z}_n, \boldsymbol{\mu}, \boldsymbol{\Omega}) \leq \ell(\mathbf{z}_1^{(0)}, \ldots, \mathbf{z}_n^{(0)}, \boldsymbol{\mu}^{(0)}, \boldsymbol{\Omega}^{(0)})\}$ is compact and that ℓ in (6) is continuous on this sublevel set. The continuity part is obvious and we just need to argue the compactness of the sublevel set. Since $\ell(\mathbf{z}_1, \ldots, \mathbf{z}_n, \boldsymbol{\mu}, \boldsymbol{\Omega})$ is a continuous function, the compactness of this sublevel set is actually implied by the coerciveness of $\ell(\mathbf{z}_1, \ldots, \mathbf{z}_n, \boldsymbol{\mu}, \boldsymbol{\Omega})$ (Calafiore and El Ghaoui, 2014, Lemma 8.3), which we are going to argue as follows.

As argued previously, $\ell(\mathbf{z}_1, \ldots, \mathbf{z}_n, \boldsymbol{\mu}, \boldsymbol{\Omega}) = \ell_0(\mathbf{z}_1, \ldots, \mathbf{z}_n, \boldsymbol{\mu}, \boldsymbol{\Omega}) + \ell_1(\mathbf{z}_1, \ldots, \mathbf{z}_n) + \ell_2(\boldsymbol{\Omega})$ as in (9)–(11). On the one hand, let's argue that $\ell_0(\mathbf{z}_1, \ldots, \mathbf{z}_n, \boldsymbol{\mu}, \boldsymbol{\Omega}) + \ell_2(\boldsymbol{\Omega})$ is bounded below as follows.

$$
\begin{aligned}
\ell_0(\mathbf{z}_1, \ldots, \mathbf{z}_n, \boldsymbol{\mu}, \boldsymbol{\Omega}) + \ell_2(\boldsymbol{\Omega}) &= -\frac{1}{2}\log[\det(\boldsymbol{\Omega})] + \frac{1}{2n}\sum_{i=1}^{n}(\mathbf{z}_i - \boldsymbol{\mu})'\boldsymbol{\Omega}(\mathbf{z}_i - \boldsymbol{\mu}) + \lambda\|\boldsymbol{\Omega}\|_1 \\
&\geq -\frac{1}{2}\log[\det\Big(\hat{\boldsymbol{\Omega}}\Big)] + \frac{1}{2n}\sum_{i=1}^{n}(\mathbf{z}_i - \boldsymbol{\mu})'\hat{\boldsymbol{\Omega}}(\mathbf{z}_i - \boldsymbol{\mu}) + \lambda\|\hat{\boldsymbol{\Omega}}\|_1 \\
&\geq -\frac{1}{2}\log[\det\Big(\hat{\boldsymbol{\Omega}}\Big)] \\
&\geq -\frac{1}{2}K\log\frac{K}{\lambda},
\end{aligned}
$$

where

$$
\hat{\boldsymbol{\Omega}} = \arg\min_{\boldsymbol{\Omega}} -\frac{1}{2}\log[\det\Big(\hat{\boldsymbol{\Omega}}\Big)] + \frac{1}{2n}\sum_{i=1}^{n}(\mathbf{z}_i - \boldsymbol{\mu})'\hat{\boldsymbol{\Omega}}(\mathbf{z}_i - \boldsymbol{\mu}) + \lambda\|\hat{\boldsymbol{\Omega}}\|_1,
$$

and the last inequality follows because $\hat{\boldsymbol{\Omega}}$ is unique and has positive eigenvalues bounded above by $\frac{K}{\lambda}$ (Banerjee et al., 2008).

On the other hand, we argue that $\ell_1(\mathbf{z}_1, \ldots, \mathbf{z}_n)$ is a coercive function of $\mathbf{z}_1, \ldots, \mathbf{z}_n$. This is because $\ell_1(\mathbf{z}_1, \ldots, \mathbf{z}_n)$ is proper, closed (as implied by continuity), strictly convex and has

a unique minimizer (with a positive definite Hessian matrix, see Section 2.3), thus every sublevel set of ℓ_1 is bounded, following Corollary 8.7.1 from Rockafellar (1970). In addition, every sublevel set of ℓ_1 is closed due to the fact that ℓ_1 is continuous (Rockafellar, 1970, Theorem 7.1). Therefore, every sublevel set of ℓ_1 is compact, implying the coerciveness of ℓ_1 (Calafiore and El Ghaoui, 2014, Lemma 8.3).

Combining that $\ell_0(\mathbf{z}_1, \ldots, \mathbf{z}_n, \boldsymbol{\mu}, \boldsymbol{\Omega}) + \ell_2(\boldsymbol{\Omega})$ is bounded below and that $\ell_1(\mathbf{z}_1, \ldots, \mathbf{z}_n)$ is a coercive function of $\mathbf{z}_1, \ldots, \mathbf{z}_n$, then if $\|(\mathbf{z}_1', \ldots, \mathbf{z}_n')\| \to \infty$, $\ell(\mathbf{z}_1, \ldots, \mathbf{z}_n, \boldsymbol{\mu}, \boldsymbol{\Omega}) \to \infty$. Thus, to show that $\ell(\mathbf{z}_1, \ldots, \mathbf{z}_n, \boldsymbol{\mu}, \boldsymbol{\Omega})$ is a coercive function, we just need to show that $g(\boldsymbol{\mu}, \boldsymbol{\Omega}) = \ell_0(\mathbf{z}_1, \ldots, \mathbf{z}_n, \boldsymbol{\mu}, \boldsymbol{\Omega}) + \ell_2(\boldsymbol{\Omega})$ is a coercive function of $\boldsymbol{\mu}$ and $\boldsymbol{\Omega}$ for fixed and finite $\mathbf{z}_1, \ldots, \mathbf{z}_n$.

Note that for fixed and finite $\mathbf{z}_1, \ldots, \mathbf{z}_n$,

$$\begin{aligned} g(\boldsymbol{\mu}, \boldsymbol{\Omega}) &= -\frac{1}{2}\log[\det(\boldsymbol{\Omega})] + \frac{1}{2n}\sum_{i=1}^{n}(\mathbf{z}_i - \boldsymbol{\mu})'\boldsymbol{\Omega}(\mathbf{z}_i - \boldsymbol{\mu}) + \lambda\|\boldsymbol{\Omega}\|_1 \\ &\geq -\frac{1}{2}\sum_{j=1}^{K}\log[\kappa_j(\boldsymbol{\Omega})] + \frac{1}{2n}\kappa_{\min}(\boldsymbol{\Omega})\sum_{i=1}^{n}\|\mathbf{z}_i - \boldsymbol{\mu}\|^2 + \lambda\kappa_{\max}(\boldsymbol{\Omega}) \\ &\geq \max(I_1, I_2), \end{aligned}$$

where $\kappa_j(\boldsymbol{\Omega})$, $\kappa_{\min}(\boldsymbol{\Omega})$, and $\kappa_{\max}(\boldsymbol{\Omega})$ denote the jth, minimum, and maximum eigenvalues of $\boldsymbol{\Omega}$, respectively, and

$$\begin{aligned} I_1 &= \frac{1}{2n}\kappa_{\min}(\boldsymbol{\Omega})\sum_{i=1}^{n}\|\mathbf{z}_i - \boldsymbol{\mu}\|^2 + \lambda\kappa_{\max}(\boldsymbol{\Omega}) - \frac{1}{2}K\log[\kappa_{\max}(\boldsymbol{\Omega})], \\ I_2 &= -\frac{1}{2}\log[\kappa_{\min}(\boldsymbol{\Omega})] + \lambda\kappa_{\max}(\boldsymbol{\Omega}) - \frac{1}{2}(K-1)\log[\kappa_{\max}(\boldsymbol{\Omega})]. \end{aligned}$$

For $L = K$ or $L = K - 1$, $\lambda\kappa_{\max}(\boldsymbol{\Omega}) - \frac{1}{2}L\log[\kappa_{\max}(\boldsymbol{\Omega})] \geq 0$ when $\kappa_{\max}(\boldsymbol{\Omega}) \to \infty$ and $\lambda\kappa_{\max}(\boldsymbol{\Omega}) - \frac{1}{2}L\log[\kappa_{\max}(\boldsymbol{\Omega})]$ is bounded below when $\kappa_{\max}(\boldsymbol{\Omega})$ is bounded above. Therefore, if $\kappa_{\min}(\boldsymbol{\Omega})$ is bounded away from 0, then $I_1 \to \infty$ when $\|\boldsymbol{\mu}\| \to \infty$ because $\frac{1}{2n}\kappa_{\min}(\boldsymbol{\Omega})\sum_{i=1}^{n}\|\mathbf{z}_i - \boldsymbol{\mu}\|^2 \to \infty$; if $\kappa_{\min}(\boldsymbol{\Omega}) \to 0$, then $I_2 \to \infty$ because $-\frac{1}{2}\log[\kappa_{\min}(\boldsymbol{\Omega})] \to \infty$. In summary, for fixed and finite $\mathbf{z}_1, \ldots, \mathbf{z}_n$, we have $g(\boldsymbol{\mu}, \boldsymbol{\Omega}) \to \infty$ when $\|\boldsymbol{\mu}\| \to \infty$ regardless of $\boldsymbol{\Omega}$.

Thus, to show that $g(\boldsymbol{\mu}, \boldsymbol{\Omega})$ is a coercive function of $\boldsymbol{\mu}$ and $\boldsymbol{\Omega}$ for fixed and finite $\mathbf{z}_1, \ldots, \mathbf{z}_n$,

it suffices to show that $g(\Omega) = \ell_0(\mathbf{z}_1, \ldots, \mathbf{z}_n, \boldsymbol{\mu}, \boldsymbol{\Omega}) + \ell_2(\boldsymbol{\Omega})$ is a coercive function of $\boldsymbol{\Omega}$ for fixed and finite $\mathbf{z}_1, \ldots, \mathbf{z}_n$ and μ. As $g(\Omega)$ is the graphical lasso objective function, it is proper, closed, convex, and has a unique minimizer (Banerjee et al., 2008; Friedman et al., 2008), thus every sublevel set of g is bounded, again following Corollary 8.7.1 from Rockafellar (1970). In addition, every sublevel set of g is closed due to the continuity of g. Therefore, every sublevel set of g is compact, implying the coerciveness of g (Calafiore and El Ghaoui, 2014, Lemma 8.3). This concludes the proof of the coerciveness of the function $\ell(\mathbf{z}_1, \ldots, \mathbf{z}_n, \boldsymbol{\mu}, \boldsymbol{\Omega})$.

Third, $\ell(\mathbf{z}_1, \ldots, \mathbf{z}_n, \boldsymbol{\mu}, \boldsymbol{\Omega})$ has at most one minimum in its second block of parameters, i.e., $\boldsymbol{\mu}$. This is because the Hessian matrix for $\boldsymbol{\mu}$ is $\boldsymbol{\Omega}$ which is positive definite.

The conclusion of Theorem 1 is thus proved as we have verified all regularity conditions in Theorem 4.1(c) in Tseng (2001). □

Simulations: Figures S1 and S2

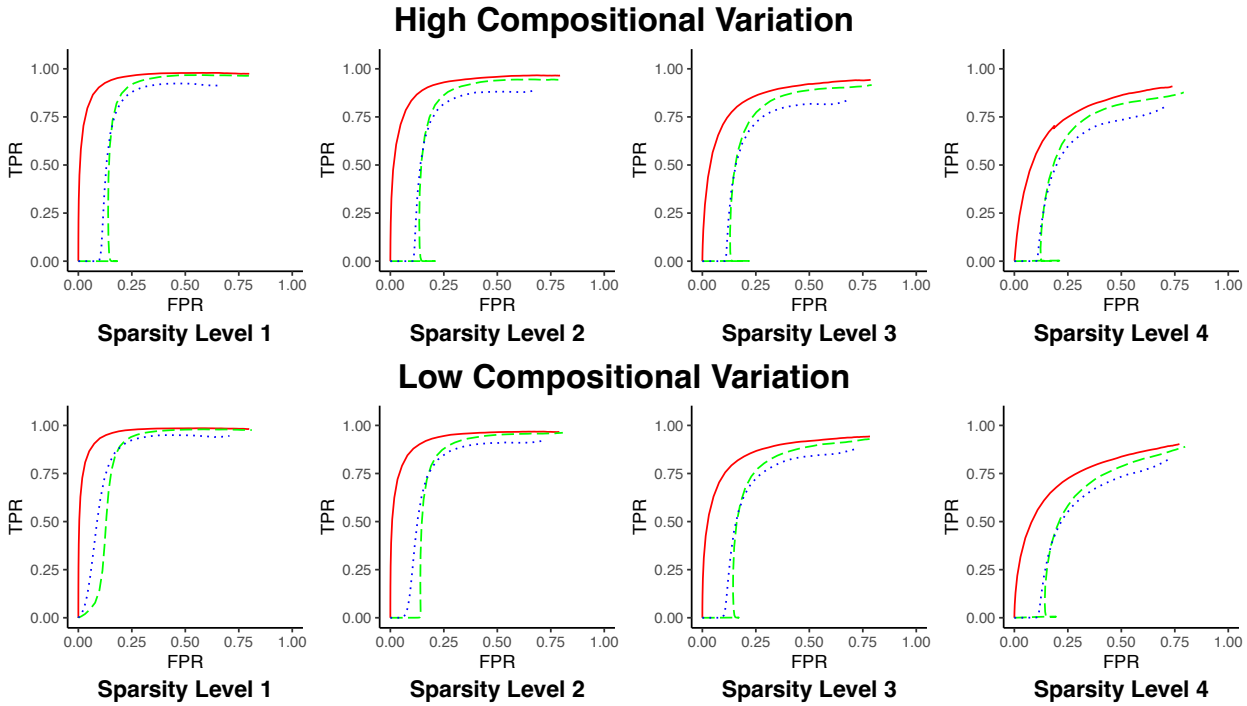

Figure S1: ROC curves for compositional graphical lasso (Comp-gLASSO), graphical lasso (gLASSO) and neighborhood selection (MB). Solid red: Comp-gLASSO; dashed green: gLASSO; dotted blue: MB. Sparsity levels 1–4: from the least sparse to the most sparse.

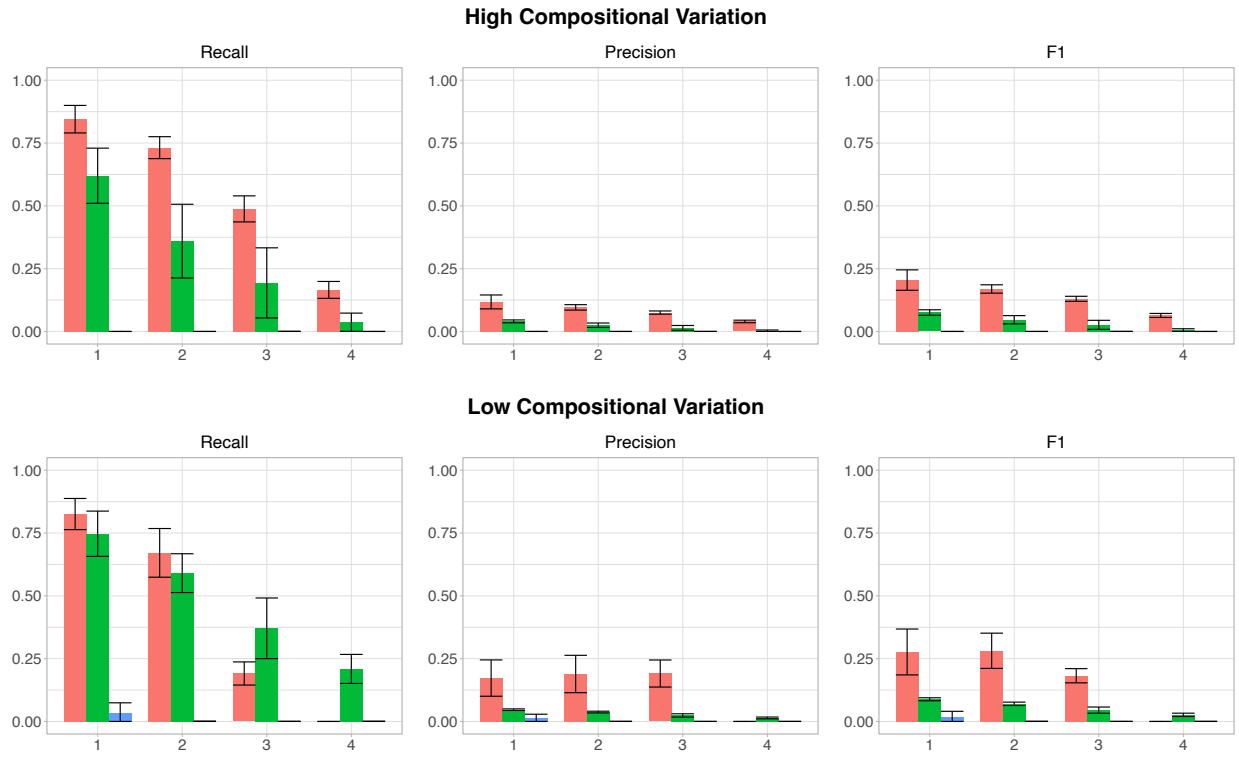

Figure S2: Recall, precision and F1 score for the network selected by StARS for compositional graphical lasso (Comp-gLASSO), graphical lasso (gLASSO) and neighborhood selection (MB). Red (left): Comp-gLASSO; green (middle): gLASSO; blue (right): MB. 1–4: sparsity levels 1–4 from the least sparse to the most sparse.

Tara Oceans Project: Additional Results

We find that compositional graphical lasso predicts a high degree for genera that are known to act as keystone species or parasitize other taxa, many of which are also high-degree in the literature validated network. For example, *Phaeocystis* elicits a high degree in both literature validated and compositional graphical lasso networks. This genus is a well-described keystone organism in some marine ecosystems (Verity et al., 2007), where it causes large phytoplankton blooms and plays an important role in the global cycling of carbon and sulfur (Verity and Smetacek, 1996). Similarly, these two networks predict a high degree for taxa that are known parasites, such as *Blastodinium* (Skovgaard et al., 2012), *Amoebophyra* (Chambouvet et al., 2008), and *Syndinium* (Skovgaard et al., 2005). In some instances, compositional graphical lasso uniquely reveals high-degree genera even when compared to the literature validated network, such as in the case of the parasite *Euduboscquella* (Bachvaroff et al., 2012), which is ranked the 5th by compositional graphical lasso but only has 1 interaction in the literature. Given the fact that the literature validated network only captures a subset of interactions that exist in nature (i.e., those interactions that have been explicitly tested), we posit that compositional graphical lasso affords an opportunity to resolve novel modulators of community composition, such as keystone taxa and generalistic parasites, that follow-up experiments can validate.

We also visualize the three genus interaction networks (from compositional graphical lasso, graphical lasso, and neighborhood selection) in company with the network of the literature validated interactions. For a better visualization, we only keep the top 100 edges that are ranked by the following two criteria: (a) selection probability, the proportion of times that an edge is selected from the N subsamples in StARS and (b) edge weight, the absolute value of the partial correlation that is defined as $|\hat{\omega}_{ij}|/\sqrt{\hat{\omega}_{ii}\hat{\omega}_{jj}}$ where $\hat{\omega}_{ij}$ is the (i, j) entry of the estimated inverse covariance matrix $\hat{\Omega}$. Specifically, the edges are first ranked by selection probability, and the edges with the same selection probabilities are further ranked by edge weight. For the networks from all three methods, darker blue implies higher magnitude in the absolute value of partial correlation.

We can see from Figure S3 that, though still different, the networks estimated by the three

algorithms have apparent similarity in the predicted edges and their edge weights, e.g., the genus pairs "*Centropages* - *Thalassicolla*" and "*Acanthometra* - *Hexaconus*" are in dark blue for all three methods. On the other hand, there are very few overlaps between those top 100 edges and the known interactions from literature. Since our current knowledge of the genus-level interactions are still limited, the edges that have not been reported from literature but enjoys higher selection probability and larger weight might suggest promising new eukaryotic interactions that deserve biological validations. There are actually 39 common edges from the top 100 edges from the three estimated networks. We provide the list of these common genus-genus interactions (Table S1) for the interested readers.

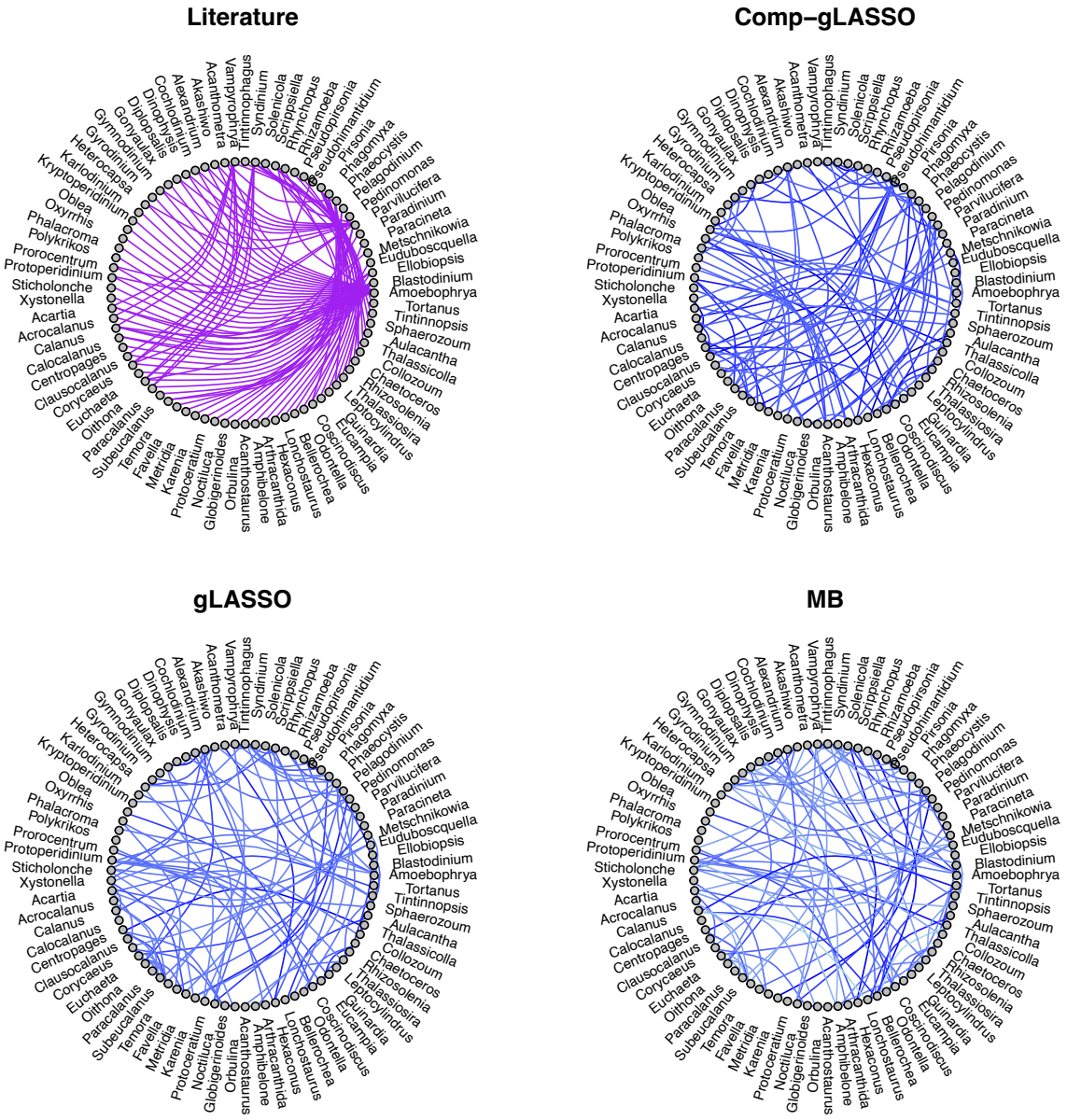

Figure S3: Inferred networks from each method with edges filtered by selection probability and ranked by edge weight, in comparison with the 91 interactions reported in literature. In each network, darker blue implies stronger (larger in absolute value) edge weight.

	Genus 1	Genus 2
1	Gonyaulax	Alexandrium
2	Thalassicolla	Centropages
3	Sphaerozoum	Collozoum
4	Hexaconus	Acanthometra
5	Pedinomonas	Karenia
6	Lonchostaurus	Aulacantha
7	Eucampia	Coscinodiscus
8	Phagomyxa	Noctiluca
9	Temora	Centropages
10	Oblea	Coscinodiscus
11	Oithona	Alexandrium
12	Orbulina	Globigerinoides
13	Vampyrophrya	Syndinium
14	Paracineta	Euchaeta
15	Tortanus	Calanus
16	Scrippsiella	Gyrodinium
17	Pseudopirsonia	Pirsonia
18	Heterocapsa	Akashiwo
19	Thalassicolla	Collozoum
20	Rhynchopus	Phaeocystis
21	Tintinnophagus	Pirsonia
22	Thalassiosira	Rhizosolenia
23	Prorocentrum	Hexaconus
24	Pseudopirsonia	Paradinium
25	Metschnikowia	Acartia
26	Leptocylindrus	Eucampia
27	Odontella	Chaetoceros
28	Globigerinoides	Corycaeus
29	Tintinnophagus	Rhynchopus
30	Metschnikowia	Aulacantha
31	Pelagodinium	Favella
32	Prorocentrum	Euduboscquella
33	Tintinnopsis	Thalassiosira
34	Collozoum	Acartia
35	Subeucalanus	Sphaerozoum
36	Vampyrophrya	Pseudohimantidium
37	Oxyrrhis	Arthracanthida
38	Temora	Acrocalanus
39	Tintinnophagus	Amoebophrya

Table S1: Genus-genus interactions that are commonly identified by compositional graphical lasso, graphical lasso, and neighborhood selection.

Zebrafish Parasite Infection Study: Additional Results

In addition to the results identified by compositional graphical lasso in the main text, we also evaluated microbial interactions by other methods in order to clarify possible interactions overlooked by compositional graphical lasso. We used the same analytic approach for all methods by first comparing the method-specific degree change for all genera between infected and uninfected hosts, identifying taxa whose degree changes substantially between treatment and control, then finally examining the biological plausibility of unique edges for these taxa according to each method.

On the one hand, findings from compositional graphical lasso encompass nearly 92% of the total edges of the neighborhood selection method for infected hosts, and 88% of the total edges for uninfected hosts. The edges which are not identified by compositional graphical lasso did not generally involve taxa whose degree varies by more than two interactions between infected and uninfected hosts, which suggests that compositional graphical lasso successfully identifies a majority of ecologically relevant edges discovered by neighborhood selection.

On the other hand, compositional graphical lasso and graphical lasso yield many similar findings regarding changes in interaction degree between infected and uninfected zebrafish hosts; compositional graphical lasso identifies 66% of the total graphical lasso edges for uninfected fish, and 74% of the edges in infected fish. Bacterial genera that show the most divergent interaction degree changes between infected and uninfected hosts for compositional graphical lasso and graphical lasso include taxa that have previously been linked to worm burden such as *Caenimonas*, *Undibacterium*, *Bosea*, and *Paracoccus*. In contrast to compositional graphical lasso, graphical lasso makes unique predictions that these microbes sustain an increased number of interactions in uninfected individuals, notwithstanding their positive association with worm burden. Graphical lasso and compositional graphical lasso also make divergent predictions regarding changes in interaction degree for taxa whose association with worm burden is not fully understood and which are typically associated with soil or plants, such as the genera *A-N-P-R* and *Ensifer*.

While compositional graphical lasso identifies many possible interactions that are sup-

ported by biological context, and predicts the majority of interactions predicted by other methods, it is likely that it does not capture every possible interaction, and experimental validation of unique predictions by other methods may help to underscore strengths of techniques like graphical lasso and limitations of the compositional graphical lasso method.

Uninfected	Infected	Uninfected	Infected	Uninfected	Infected
Comp-gLASSO		gLASSO		MB	
Plesiomonas (21)	Photobacterium (19)	Silvanigrella (21)	Paucibacter (21)	Rheinheimera (9)	Fluviicola (7)
Paraclostridium (18)	Weissella (18)	Peptostreptococcus (21)	Phreatobacter (18)	Aeromonas (8)	Aeromonas (6)
Aeromonas (17)	Gemmobacter (18)	Aeromonas (20)	Fusobacterium (17)	Cetobacterium (8)	Paucibacter (5)
Paucibacter (17)	Fusobacterium (17)	Plesiomonas (20)	Cetobacterium (16)	Runella (6)	Runella (5)
Photobacterium (16)	Paucibacter (15)	Paraclostridium (19)	Cloacibacterium (16)	Peptostreptococcus (6)	Cetobacterium (4)
Fusobacterium (16)	Yersinia (15)	Pseudoduganella (18)	Weissella (16)	Pseudomonas (5)	Paraclostridium (4)
Lactobacillus (16)	Crenobacter (14)	Rheinheimera (18)	ZOR0006 (15)	Cloacibacterium (5)	Yersinia (4)
Rheinheimera (15)	Aurantisolimonas (14)	Bacteroides (18)	Flavobacterium (15)	Photobacterium (5)	Fusobacterium (4)
Yersinia (15)	Paracoccus (14)	Undibacterium (17)	Yersinia (15)	Haliscomenobacter (5)	Paracoccus (4)
Silvanigrella (15)	Ignatzschineria (14)	Photobacterium (17)	Shewanella (14)	Tychonema (5)	Ignatzschineria (4)
Bacteroides (15)	Lysinibacillus (14)	Runella (17)	Aurantisolimonas (14)	Plesiomonas (4)	Bosea (4)
Chitinibacter (14)	Plesiomonas (13)	Paucibacter (16)	Aeromonas (13)	Acinetobacter (4)	Bacteroides (4)
Weissella (14)	Acinetobacter (13)	Chitinimonas (16)	Acinetobacter (13)	Paucibacter (4)	Pseudomonas (3)
Paracoccus (14)	Chitinibacter (13)	Yersinia (16)	Crenobacter (13)	Shewanella (4)	Chitinibacter (3)
Peptostreptococcus (14)	Rheinheimera (13)	Paracoccus (16)	A-N-P-R (13)	Pseudoduganella (4)	Crenobacter (3)
Pseudomonas (13)	Cetobacterium (12)	Caenimonas (16)	Pseudoduganella (12)	Chitinimonas (4)	ZOR0006 (3)
Acinetobacter (13)	Cloacibacterium (12)	Lactobacillus (16)	Caenimonas (12)	Fluviicola (4)	Pseudoduganella (3)
Pseudoduganella (13)	Phreatobacter (12)	Luteimonas (15)	Gemmobacter (12)	Aurantisolimonas (4)	Cloacibacterium (3)
Cloacibacterium (13)	Tychonema (12)	Ignatzschineria (15)	Ignatzschineria (12)	Fusobacterium (4)	Photobacterium (3)
Chitinimonas (13)	Bacteroides (12)	Lysinibacillus (15)	Lysinibacillus (12)	Caenimonas (4)	Chitinimonas (3)
Ignatzschineria (13)	Aeromonas (11)	Cetobacterium (14)	Lactobacillus (12)	Defluviimonas (4)	Aurantisolimonas (3)
Lysinibacillus (13)	Shewanella (11)	Chitinibacter (14)	Pseudomonas (11)	Ensifer (4)	Phreatobacter (3)
Shewanella (12)	Undibacterium (11)	Shewanella (14)	Chitinibacter (11)	Bosea (4)	Defluviimonas (3)
ZOR0006 (12)	Chitinimonas (11)	Cloacibacterium (14)	Mycoplasma (11)	Chitinibacter (3)	Tychonema (3)
Flavobacterium (12)	Lactobacillus (11)	Phreatobacter (14)	Photobacterium (11)	Crenobacter (3)	Peptostreptococcus (3)
Mycoplasma (12)	ZOR0006 (10)	Gemmobacter (14)	Fluviicola (11)	Flavobacterium (3)	Plesiomonas (2)
Tychonema (12)	Pseudoduganella (10)	Bosea (14)	Rheinheimera (11)	A-N-P-R (3)	Acinetobacter (2)
Undibacterium (11)	A-N-P-R (10)	Tychonema (14)	Paracoccus (11)	Luteimonas (3)	Undibacterium (2)
Crenobacter (10)	Mycoplasma (9)	Pseudomonas (13)	Runella (11)	Paracoccus (3)	Flavobacterium (2)
Fluviicola (10)	Fluviicola (9)	Acinetobacter (13)	Haliscomenobacter (11)	Gemmobacter (3)	Weissella (2)
Defluviimonas (10)	Luteimonas (9)	A-N-P-R (13)	Bosea (11)	Lysinibacillus (3)	Rheinheimera (2)
Ensifer (10)	Defluviimonas (9)	Fluviicola (13)	Plesiomonas (10)	ZOR0006 (2)	Luteimonas (2)
Cetobacterium (9)	Ensifer (9)	Weissella (13)	Undibacterium (10)	Undibacterium (2)	Gemmobacter (2)
A-N-P-R (9)	Peptostreptococcus (9)	ZOR0006 (12)	Paraclostridium (10)	Weissella (2)	Ensifer (2)
Aurantisolimonas (9)	Pseudomonas (8)	Flavobacterium (12)	Chitinimonas (10)	Yersinia (2)	Haliscomenobacter (2)
Luteimonas (9)	Flavobacterium (8)	Mycoplasma (12)	Defluviimonas (10)	Phreatobacter (2)	Lactobacillus (2)
Runella (9)	Caenimonas (8)	Defluviimonas (12)	Ensifer (10)	Ignatzschineria (2)	Mycoplasma (1)
Haliscomenobacter (9)	Haliscomenobacter (8)	Haliscomenobacter (12)	Tychonema (10)	Lactobacillus (2)	A-N-P-R (1)
Caenimonas (8)	Bosea (8)	Crenobacter (11)	Silvanigrella (10)	Mycoplasma (1)	Lysinibacillus (1)
Gemmobacter (8)	Silvanigrella (8)	Aurantisolimonas (10)	Luteimonas (9)	Paraclostridium (1)	Silvanigrella (1)
Bosea (8)	Paraclostridium (6)	Fusobacterium (10)	Peptostreptococcus (9)	Silvanigrella (1)	Shewanella (0)
Phreatobacter (7)	Runella (5)	Ensifer (9)	Bacteroides (9)	Bacteroides (1)	Caenimonas (0)

Table S2: The ranks of genera in each degree distribution (in descending order) for uninfected fish and infected fish separately, from compositional graphical lasso (Comp-gLASSO), graphical lasso (gLASSO), and neighborhood selection (MB). The numbers in the parentheses are the corresponding degrees of the genera.